Characterisation of Al–Ti dissimilar material joints fabricated using ultrasonic additive manufacturing

P. J. Wolcott[1], N. Sridharan[2], S. S. Babu[2], A. Miriyev[3], N. Frage[3] and M. J. Dapino*[1]

Ultrasonic additive manufacturing (UAM) is a solid state manufacturing process for joining thin metal tapes using principles of ultrasonic metal welding. The process operates at low temperatures, enabling dissimilar material welds without generating harmful intermetallic compounds. In this study, a 9 kW UAM system was used to create joints of Al 1100 and commercially pure titanium. Viable process parameters were identified through pilot weld studies via controlled variation of weld force, amplitude and weld speed. Push-pin delamination tests and shear tests were performed, comparing as-built, heat treated and spark plasma sintering treated samples. Heat treated and spark plasma sintering treated samples yielded mechanical strengths over twice that of as-built samples. Electron backscatter diffraction measurements show that deformation and grain refinement only take place in the aluminium layers. Heat treated samples exhibit a thin intermetallic layer, which is hypothesised as constraining the interface, leading to the improved strength.

Keywords: Ultrasonic additive manufacturing, Metal matrix composites, Ultrasonic welding, Dissimilar joining, Post-treatment

Introduction

Ultrasonic additive manufacturing (UAM) is a low temperature manufacturing process that uses cyclic interface deformation developed via piezoelectric transducers to generate solid state welding, following principles of ultrasonic metal welding. Generally, the materials being welded are thin metal foils, on the order of 150 μm thick, welded onto a baseplate, or subsequent foil layers. The cyclic motion generated by the piezoelectric transducers operates at the system natural frequency, often 20 kHz. This cyclic motion, combined with a normal force acting on the foil, collapses asperities and creates plastic deformation at the weld interface.[1] These processes generate nascent metal surfaces, as well as recovery and recrystallisation at the interface, which produces metallurgical bonding. The process works in a continuous rolling action, allowing tapes to be laid along a specified path. Following a weld pass, foils can be laid either on top of or next to the previous weld. Certain UAM systems are equipped with computer numerical control (CNC) machining capabilities as well, allowing for unique shapes and geometries to be achieved through the tandem use of additive and subtractive stages. Example applications include unique channel geometries for thermal management devices and embedded active materials within a composite structure.[2,3]

The higher temperatures associated with fusion based processes can promote diffusion and intermetallic formation in dissimilar material combinations. Because the UAM process operates at temperatures below melting and the heat generated is quickly dissipated, harmful intermetallics are not generated at the interface.[4] This allows dissimilar material combinations to be welded without significant degradation in material properties. Previously successful combinations include Al–Ti, Al–Cu, Al–Ni and others.[5] These dissimilar material combinations can be used for cladding applications, composites with controlled material properties and others. While intermetallics are not generated at the surface during welding, post-process heat treatments can be performed to improve bonding through controlled generation of intermetallics, which constrain the bond area, increasing mechanical strength.[6]

Recent developments in the UAM process have increased the available weld power from 1 to 9 kW. These advances allow normal forces on the order of up to 12 000 N to be applied, as well as increasing the possible vibration amplitudes from 30 to 50 μm for welding. The maximum normal force achievable for 1 kW systems was 1000 N. The increased power in 9 kW systems has led to the generation of void less joints and increases in mechanical strength as compared to joints

[1]Department of Mechanical and Aerospace Engineering, The Ohio State University, Columbus, OH 43210, USA
[2]Department of Mechanical, Aerospace, and Biomedical Engineering, University of Tennessee, Knoxville, TN 37996, USA
[3]Department of Materials Engineering, Ben-Gurion University of the Negev, Beer Sheva 84105, Israel

*Corresponding author, email dapino.1@osu.edu

Published by Maney on behalf of the Institute
Received 30 April 2015; accepted 25 June 2015
DOI 10.1179/1362171815Y.0000000072

with 1 kW systems, which could have as much as 25% void content and tensile strengths reaching 15% of bulk material.[7,8] It has likewise expanded the weldable material envelope into materials such as copper alloys that were difficult to achieve using 1 kW UAM.[4]

Various aspects of Ti/Al joining have been examined with 1 kW UAM. Using a shear testing and 1 kW UAM, Hopkins *et al.*[9] identified optimal process parameters for joining Cp Ti and Al 1100, examining the shear strength and tensile strength of multimaterial builds. Studies by Obielodan *et al.*[10] examined joints of Cp Ti and Al 3003, which exhibited as-built shear strengths of 34 MPa. Their work also showed that shear strengths of up to 73 MPa can be achieved through use of a post-process heat treatment, which induces diffusion.

These works have shown the promise of applying the UAM process to joining Al–Ti structures; however, the shear strengths achieved are less than the shear strength of cold worked Al 1100 (90 MPa),[11] and detailed investigations of the microstructure using electron backscatter diffraction (EBSD) of such joints is lacking. The focus of this work is the application of the 9 kW UAM process and its effect on the mechanical and microstructural properties of Al–Ti joints. With the enhancements associated with the 9 kW process, such as increased applied amplitudes and normal forces, increases in bond strengths are expected. Specific areas of interest are the mechanical strength of Al–Ti joints both in the as-built and heat treated conditions and the microstructural effects of post-process heat treatments.

Additionally, with the recent successful experience in joining dissimilar materials using spark plasma sintering (SPS),[12] SPS was used as a post-joining treatment. Mechanical strength is examined via delamination strength and shear testing. Microstructural aspects are examined via scanning electron microscopy (SEM), including EBSD.

Experimental

Sample manufacturing

All welds in this study were performed with a Fabrisonic SonicLayer 4000 9 kW UAM system. The system is fully automated with welding and subtractive milling capabilities. Al 1100 foils and commercially pure titanium foils 0.005 in (0.127 mm) thick were used in this study. Nominal compositions and ultimate tensile strengths for these materials are given in Table 1. During joining, a bilayer arrangement is used where titanium on top of aluminium is welded in one step. This is shown schematically in Fig. 1. In this arrangement, the sonotrode is in contact with the titanium layer only. All samples were built onto a solid aluminium 6061-T6 baseplate with the Al 1100/Al 6061 interface as the first layer.

Previous work in 1 kW UAM proved joining of Ti–Al builds and identified optimal build parameters using a design of experiments approach for Cp Ti and Al 1100.[9] With the developments associated with 9 kW UAM, specifically increases in applied amplitude, it is necessary to re-examine these parameters, as 9 kW UAM has exhibited improvements in bond quality for other material systems.[7] Weld amplitude has been shown to provide increased bond strength for both 1 and 9 kW UAM.[7–9]

Pilot studies were performed to identify the viable weld parameters for Ti–Al builds. Weld trials were conducted using the bilayer arrangement on an aluminium 6061-T6 baseplate while varying process parameters including weld force, weld amplitude, weld speed and baseplate temperature. Weld trials were considered successful when the material bonded to the baseplate and could not be pulled off manually. In most trials, Al 1100 would bond well to the Al 6061 baseplate; however, achieving a successful bond of titanium to Al 1100 was more difficult. The successful process parameters for Ti–Al from pilot studies is shown in Table 2. These parameters were used for all builds performed in this study.

Joint characterisation

Following joint construction, builds were examined for their mechanical performance as well as microstructure. Mechanical performance was investigated via push-pin and shear testing. The push-pin test is a comparative test that provides a metric of bond strength via delamination of a build. The test was originally proposed by Zhang *et al.*[13] and has proven viable in other studies.[6,7] This test is used instead of a traditional tensile test because it provides a measurement of the bond strength in a relatively small number of layers, significantly reducing costs. Likewise, the samples are easily machined using the UAM system and three-axis mill. More details on the test can be found in the work by Zhang *et al.*[13] Builds for the tests were constructed using five Ti–Al bilayers, totalling ten layers, with a hole machined through the base layer to the first layer of aluminium. This is the first layer tested, though as the test progresses the pin presses through to other layers as well. Push-pin tests were performed using a Gleeble 3800 thermo-mechanical test frame at room temperature. During the test, a pin is pressed through the sample at 0.2 mm s^{-1} with the load and displacement being recorded. A schematic of the test specimen and implementation into the Gleeble machine are presented in Fig. 2. The maximum force of the pushout as well as the area under the curve, or mechanical work, are the two metrics used to analyse the results of the test.

Following construction of the push-pin samples, designated builds were heat treated to examine the effect of heat treatment on mechanical and microstructural properties. Heat treatments were performed in a conventional induction furnace in an air atmosphere at 600°C for 1 h, following previous works.[14,15] The work by Kim and Fuji in friction welding of Al–Ti combinations has shown that this treatment optimises tensile

Table 1 Nominal composition (wt-%) and ultimate tensile strength (UTS) of materials

Material	C	H	O	N	Fe	Ti	UTS/MPa
Cp Ti	0.10	0.015	0.25	0.03	0.25	Balance	343
Material	**Si**	**Cu**	**Mn**	**Zn**	**Residuals**	**Al**	**UTS/MPa**
Al 1100-O	1.0	0.05–0.20	0.05	0.10	0.15	99.0 min	90

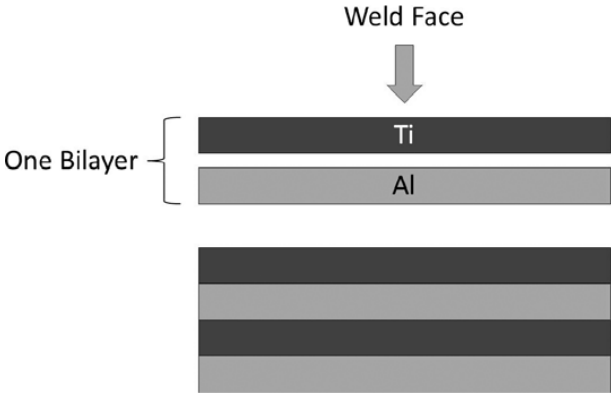

1 Arrangement for Ti–Al bilayers

Table 2 Weld parameters used for Ti–Al joints

Parameter	Level
Weld force	3500 N
Weld speed	60 in min^{-1} (25.4 mm s^{-1})
Amplitude	41.55 μm
Temperature	200°F

strength and elongation while also producing material failures away from the joint interface.

Shear testing was conducted on samples of 16 bilayers, totalling 32 total layers, sectioned into 5 × 5 mm samples and mounted in a specially designed test module. The test set-up ensures that shear occurs within the layered structure and not through the aluminium baseplate material. Specimens were tested using a 50 kN Lloyd mechanical test frame where load was applied until failure. Figure 3 shows the sample and the sample within the test fixture. Shear testing was conducted on as-built and SPS treated samples. Spark plasma sintering treatment (FCT System, Rauenstein, Germany) was conducted at 500°C for 600 s under argon atmosphere (10^{-2} torr) and uniaxial pressure of 15 MPa.

In addition to mechanical testing, microstructural evaluations were performed. Optical microscopy was used to determine if significant voids were present in the builds. Scanning electron microscopy was used to further examine the builds including a chemical analysis to measure diffusion; EBSD was used to investigate the grain structure of the resulting joints. Samples for microstructural analyses were sectioned perpendicular to the welding direction and mounted in epoxy. Grinding was performed using 180, 320, 400, 600, 800 and 1200 grit papers. Polishing was performed with 3 and 1 μm diamond pastes, finished with a 0.5 μm colloidal silica solution.

Results

Push pin testing

A summary of the results of push-pin testing is presented in Table 3, including both as-built and heat treated samples. The individual curves for each of the tests is shown in Fig. 4. The maximum force during delamination and the mechanical work, or area under the force–displacement curve, were used as metrics for examining the results of the testing. As can be seen, the results for the heat treated samples yield much higher values of delamination force, ~2.4 versus 5.8 kN on average. Similarly, the mechanical work for failure is significantly higher for heat treated samples, roughly 3.5 versus 12.7 kN-mm on average. These results indicate that heat treatment significantly increases the mechanical strength of Al–Ti bonded samples. The variation within the as-built and heat treated test groups is attributed to variations in machining and heat treatment, causing slight changes in the mechanical strength within a specific group.

Images of the fractured push-pin samples are shown in Fig. 5. The as-built samples are observed to fail by delamination of a single layer along the entire bonded area with some delamination in the higher layers, indicating that the bond strength is lower than the material strength. By contrast, the heat treated samples fail through multiple layers as shown by the concentric rings in Fig. 5*b*, indicating that the bond can withstand significant loading before failure of the tape material. These failure rings are likewise more consistent and uniform than the small amounts of delamination in the as-built samples. The discrete jumps in the load–displacement curves in Fig. 4 correlate with the fracture of specific layers within the bonded sample. These jumps are present in both heat treated samples but are absent in the as-built samples, indicating a difference in their failure behaviour.

An SEM image of the fracture surface of an as-built push-pin sample is shown in Fig. 6*a*. The image shows some degree of ductile failure surrounded by areas of

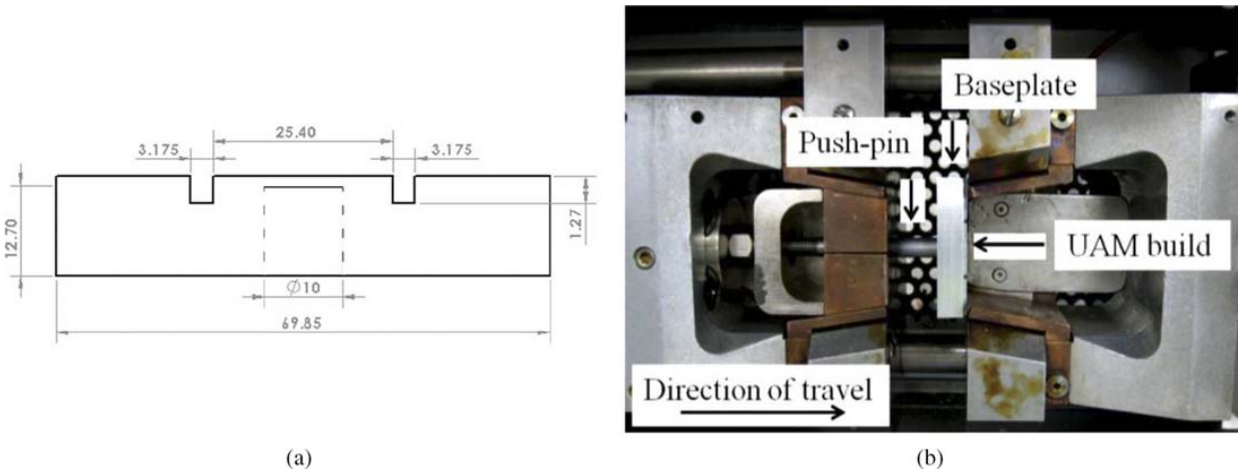

2 *a* sample dimensions (in mm) and *b* arrangement within Gleeble for push-pin test[6]

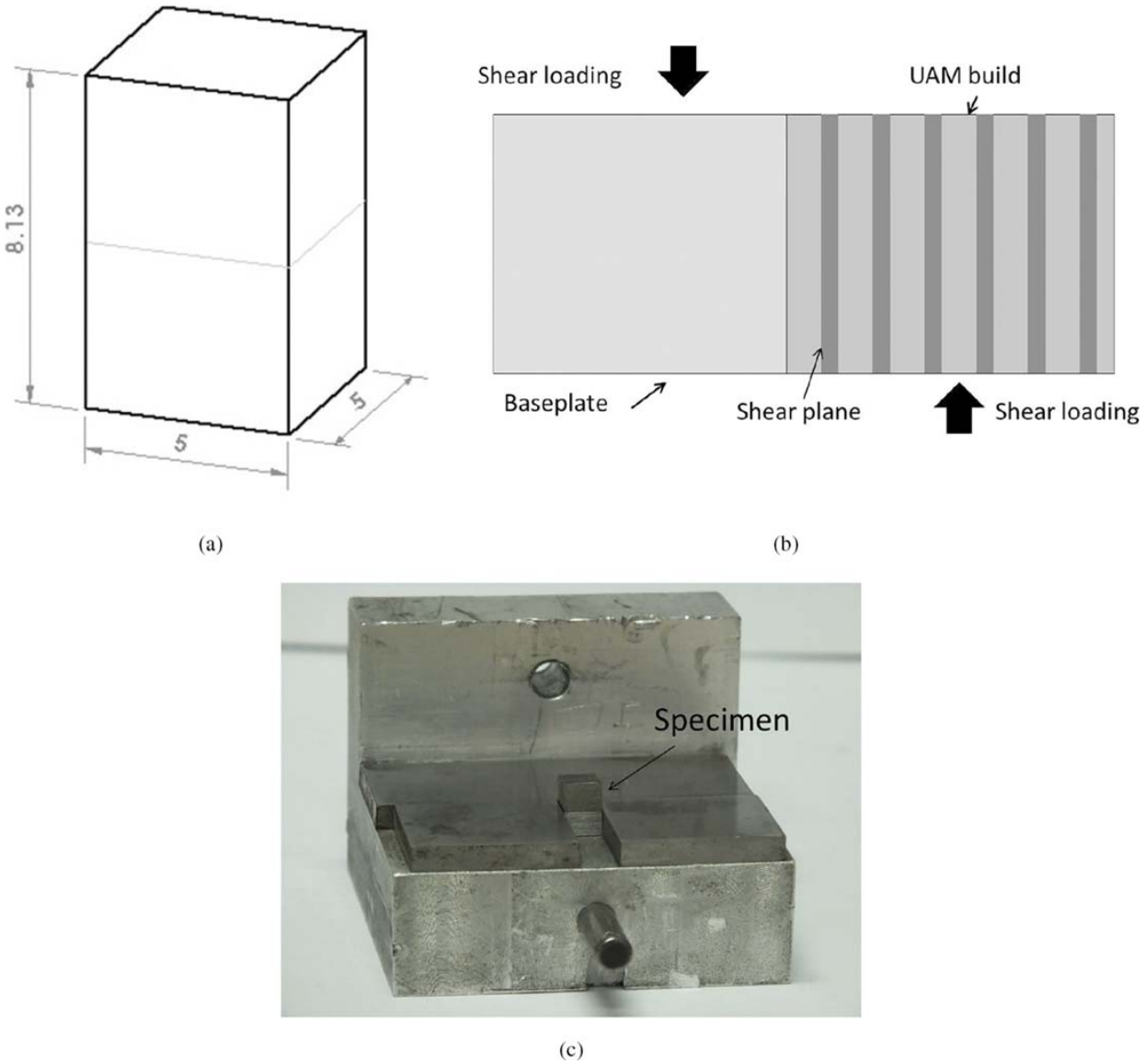

3 Set-up for shear test including *a* shear specimen drawing (in mm), *b* schematic of shear test loading conditions (not to scale) and *c* image of shear fixture

material contact, without ductile failure. Energy dispersive spectroscopy (EDS) maps of the Al and Ti content are provided in Fig. 6*b* and *c* showing the elemental content in these areas. While the failure is primarily in the aluminium, areas of titanium are present surrounding the ductile failure indicating a material transfer is occurring during bonding.

Shear testing

Results of shear testing are summarised in Table 4 showing the average ultimate shear stress and standard deviation of the tests. As is shown, the shear strength of the SPS treated samples exhibits ultimate shear strengths over two times that of the as-built samples with strengths of 46.3 versus 102.4 MPa. Additionally, the failure characteristics of the as-built and heat treated samples

Table 3 Results of push-pin testing

Sample	Force/kN	Mechanical work/kN-mm
As-built 1	2.27	2.66
As-built 2	2.5	4.42
Heat treated 1	5.05	12.09
Heat treated 2	6.5	13.4

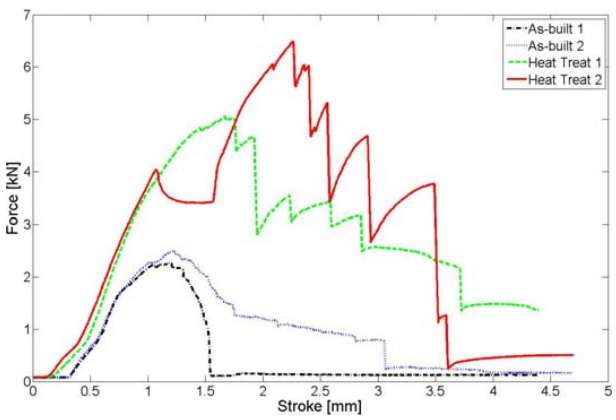

4 Push-pin data

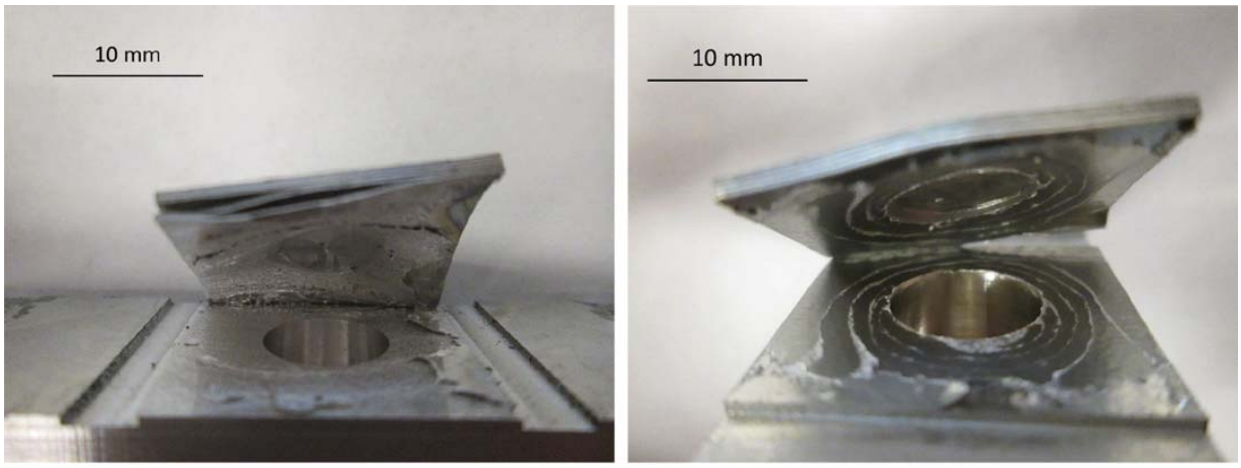

5 Failure surfaces of push-pin samples for *a* as-built and *b* heat treated samples

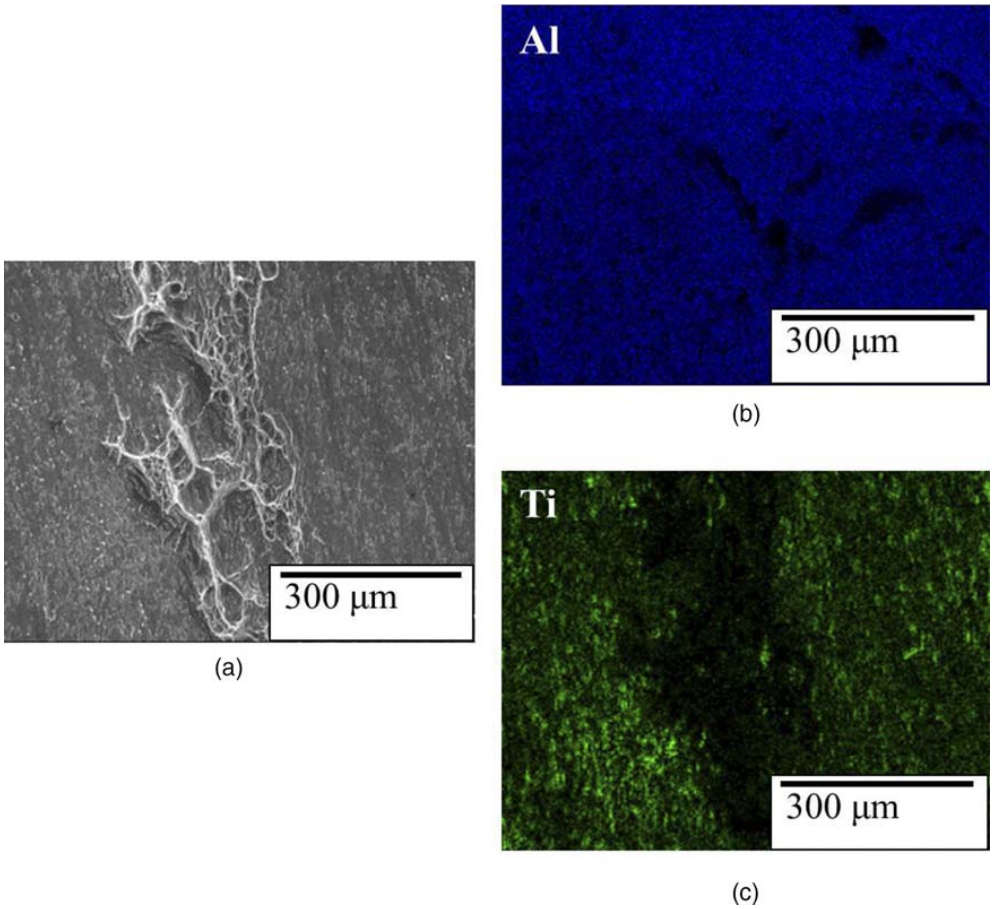

6 *a* image (SEM) of failure surface of as-built push-pin sample, *b* EDS mapping of Al and *c* EDS mapping of Ti

exhibit contrasting behaviour. Figure 7 shows failed shear specimens for each case. The as-built sample broke into separate parts, while the heat treated samples exhibited a more ductile failure.

Table 4 Results of shear testing

Condition	Average ultimate shear stress/MPa	Standard deviation/ MPa
As-built	46.3	2.6
Heat treated	102.4	7.4

The surfaces of fractured specimens were examined under optical microscopy, shown in Fig. 8. The textured surface exhibited by the as-built sample is indicative of brittle failure, whereas the gliding texture shown by the heat treated sample is indicative of a more ductile failure mechanism. The striations seen in Fig. 8*b* suggest that a smearing or sliding action is occurring during loading, which is due to the ductile nature of the failure, while the brittle failures shown in Fig. 8*a* lack these striations. These results, along with the shear strength results, indicate that heat treatment can significantly increase the strength and ductility of Al–Ti joints.

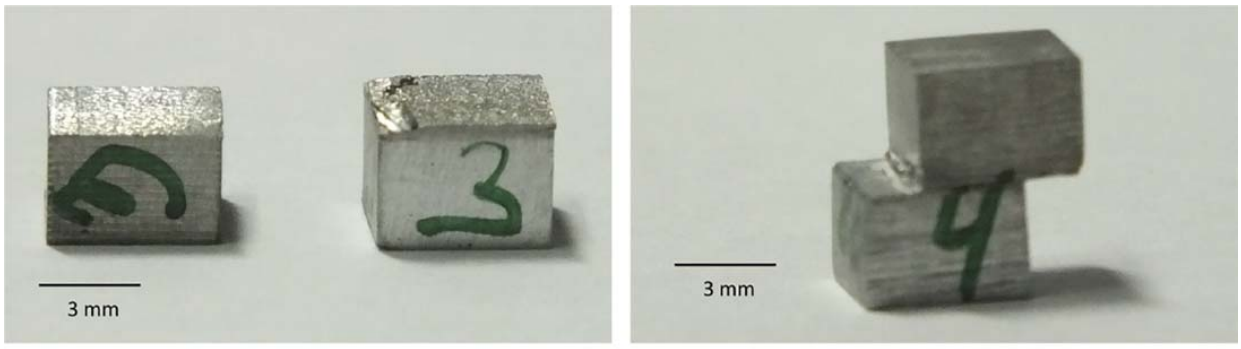

a as-built; *b* heat treated

7 Failed shear test specimens

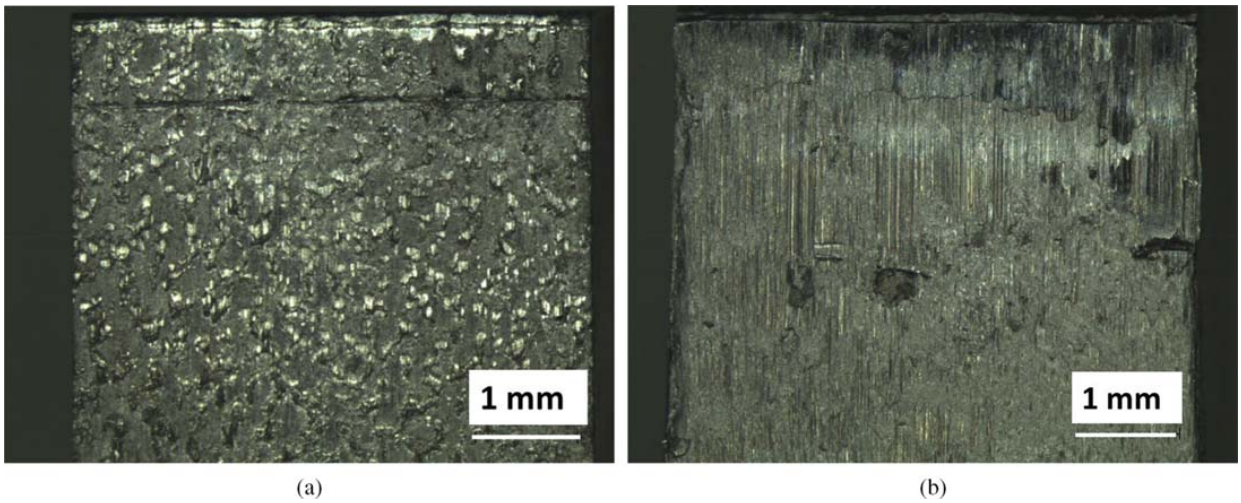

a as-built; *b* heat treated

8 Failed shear test specimens

Microstructural evaluations

Evaluation of the cross-section of an as-built Ti–Al sample is shown in Fig. 9*a*, where no indications of large voids in the sample are present. In addition, it can be seen that the top of the titanium layers have an imparted roughness from the sonotrode, while the bottom of each titanium layer contains a smooth to smooth interface with the aluminium. This imparted roughness could play a role in how the two materials are joining, especially if the bond mechanism is mechanical interlocking, which has been shown in previous studies.[9]

To investigate the chemistry along the interfaces, a diffusion profile was investigated along the line shown Fig. 9*a*. The diffusion profile for the full line scan and for the first Al–Ti interface layer are shown in Fig. 9*b* and *c* respectively. As can be seen, there is no large scale diffusion of aluminium or titanium into the adjoining material.

Fig. 10 shows the EBSD scan of an as-built Ti–Al build. Results show significant deformation in the aluminium layers at the titanium/aluminium interfaces. The aluminium layers have a nominal thickness of 127 μm before welding, which is reduced to ~70 μm after the UAM process. By contrast, the titanium layers are nominally 127 μm before welding and 125 μm after welding. The layers lower in the build show more grain refinement and deformation than layers further up the build. Figure 11 shows the grain structure of the titanium foil before welding. Comparing this with Fig. 10, it appears that the microstructure in the titanium is unchanged during the welding process, with all deformation and refinement occurring in the softer aluminium layers.

Heat treated samples were also investigated for their microstructure. An SEM image of a smooth interface of a heat treated Ti–Al sample is shown in Fig. 12*a*, where a transition zone exists between the aluminium and titanium. To investigate the chemistry within this zone, a diffusion profile was measured, shown in Fig. 12*b*. These results show that significantly more diffusion is occurring in the heat treated sample than in the as-built samples, with a diffusion zone of roughly 5 μm. A diffusion scan of an interface that was roughened by the sonotrode during welding is presented in Fig. 13.This roughened interface shows ~6 μm of diffusion across the interface, slightly more than the smooth interface, indicating that a roughened texture may induce more diffusion after heat treatment.

Measurements by EBSD for a heat treated Ti–Al sample are shown in Fig. 14. The grain structure in the titanium layers appears unchanged compared to the as-built samples, while the aluminium layers show

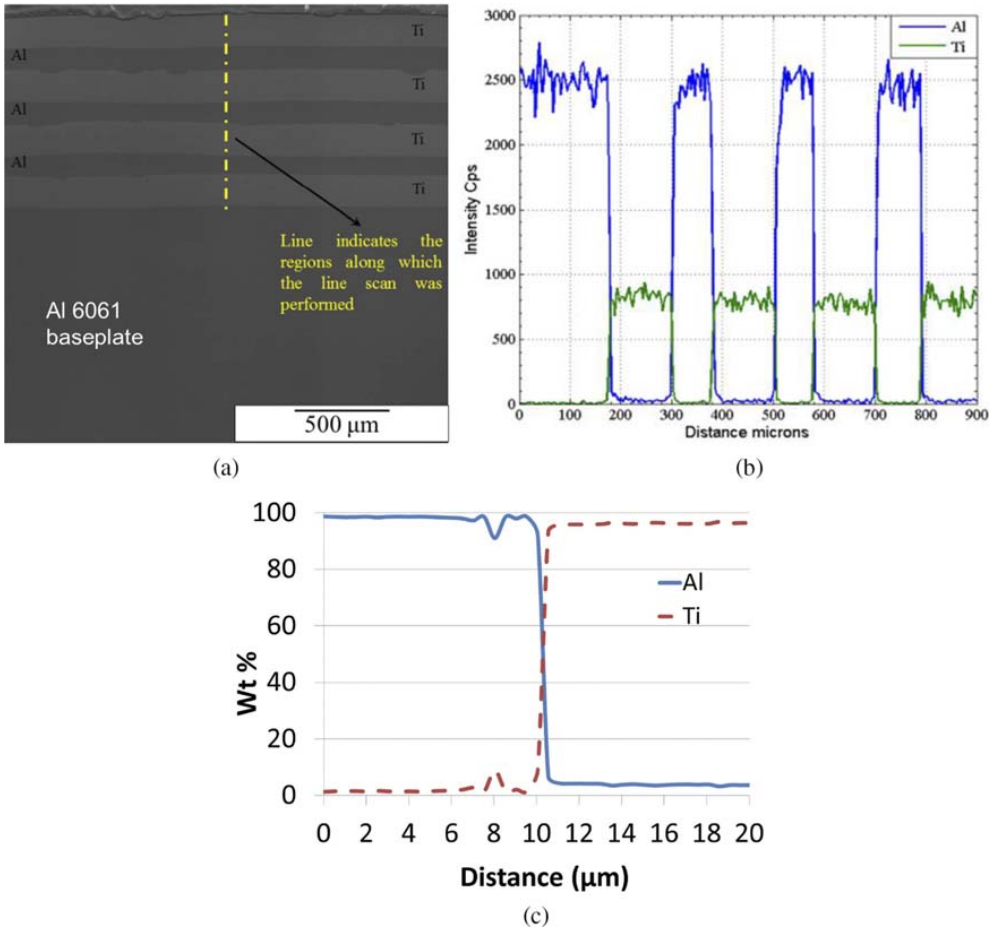

9 ***a*** **image (SEM) showing diffusion line scan for as-built Al–Ti sample and** ***b***, ***c*** **results of scan at different scales**

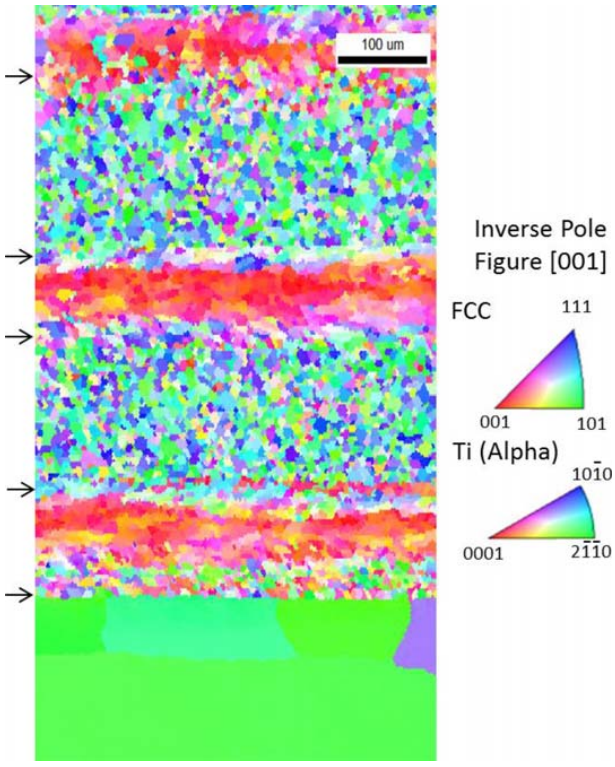

10 Electron backscatter diffraction image of Ti–Al joint; arrows indicate approximate location of material interfaces

significant grain growth. In each of the aluminium layers, it appears the heat treatment has caused preferential grain growth into only a few grains for each layer. Grain growth in the substrate Al 6061 material appears as well, though not to the extent of the growth in Al 1100 layers.

Discussion

Push-pin testing shows that post-process heat treatment of Ti–Al builds produces significant increases in mechanical strength, as measured by the mechanical work for failure. Increases from 3.5 to 12.7 kN-mm were exhibited when applying a post-process heat treatment. Differences were present in the failure surfaces as well. Heat treated specimens failed through multiple layers, while as-built samples failed mostly by delamination of a single layer. The complex stress states of the test can make it difficult to differentiate the exact loading conditions during and immediately before failure, making it difficult to discern the local failure behaviour. However, failure through multiple layers indicates strong bonding is occurring, which can withstand the push-pin load until fracture of the material occurs. After failure, the load is redistributed to the layers above and continued until the sample completely fails. When weaker bonding is occurring, as in the as-built case, delamination occurs because the weak bonding in a given layer is unable to withstand the push-pin forces, indicating that

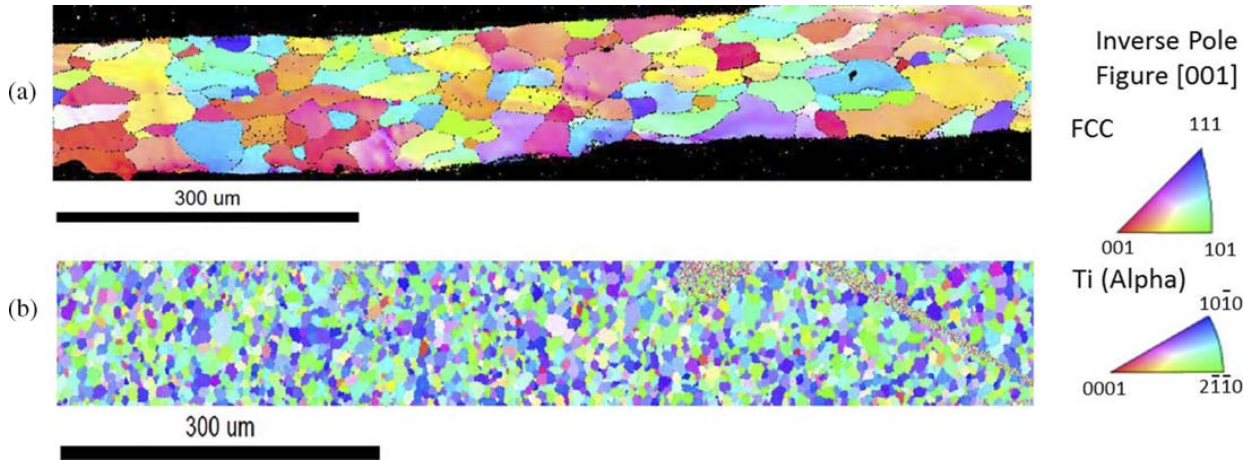

11 Electron backscatter diffraction image of *a* Al foil and *b* Ti foil, before welding

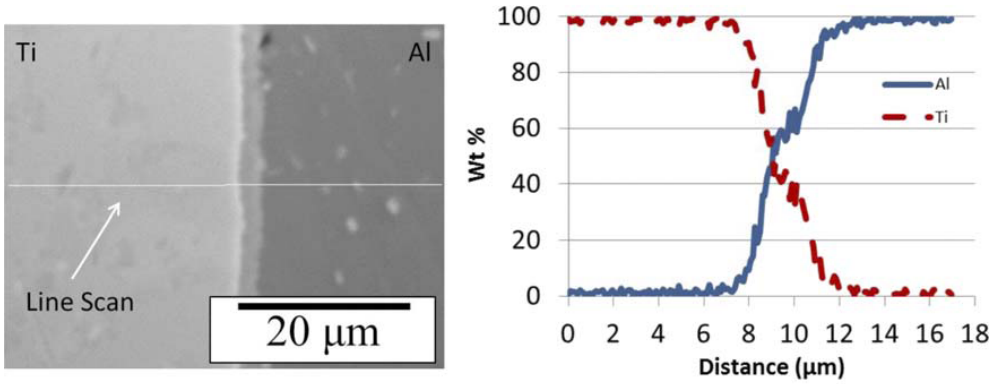

12 Diffusion line scan for Ti–Al after heat treatment along smooth interface

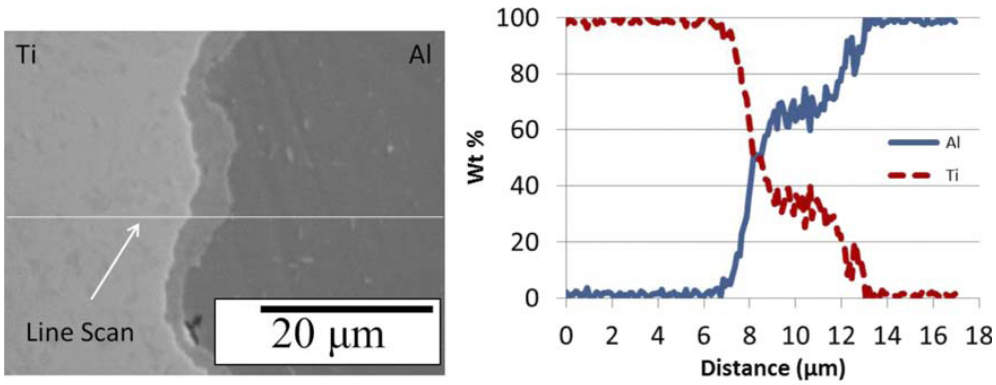

13 Diffusion line scan for Ti–Al after heat treatment along interface roughened by sonotrode

the bond strength along the layer surface is weaker than the material itself.

Similarly, shear tests show a strength increase from 46.3 to 102.4 MPa from as-built to heat treated samples. Microstructural investigations show that an intermetallic layer of ~5 μm is forming between the titanium and aluminium layers after heat treatment. It is hypothesised that this thin intermetallic layer is biaxially constrained by the layers on each side of the interface. Conceptually, this is similar to what can occur during brazing where a thin braze layer constrains the interface, preventing plastic deformation in the braze zone, increasing mechanical strength.[16] In this case, the intermetallic layer acts similarly to the thin braze layer, and the biaxial stress state achieved leads to increases in mechanical strength. This strengthening effect from an intermetallic layer has been observed in the joining of Al–Cu samples.[6,17] This phenomenon is expected to be the cause of the increases in shear strength and push-pin strength observed. Slightly higher diffusion zones of 6 μm are observed for interfaces roughened by the sonotrode. This could indicate that the amount of diffusion occurring during heat treatment can be controlled by the amount of surface roughness imposed during welding. This effect will require further investigation.

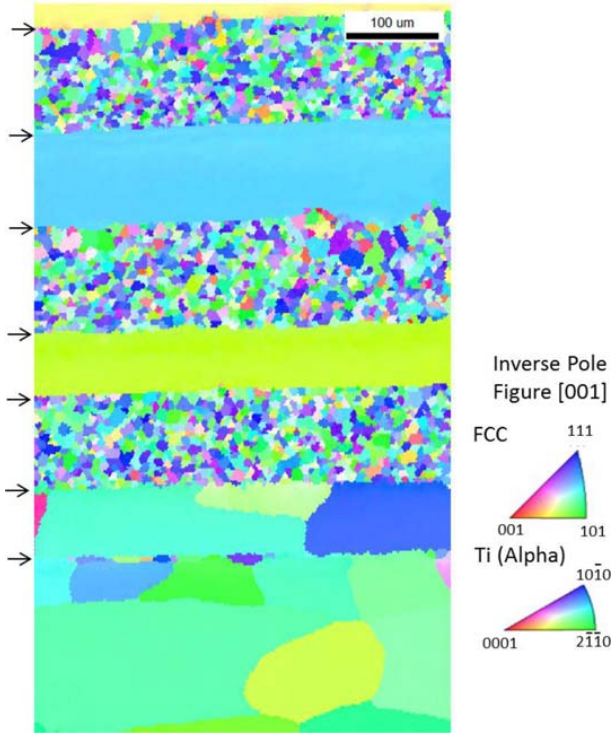

14 Electron backscatter diffraction image of Ti–Al joint after heat treatment; arrows indicate approximate location of material interfaces

Previous studies have examined various aspects of Ti/Al joining using 1 kW UAM. Using a modified shear test set-up and 1 kW UAM, Hopkins *et al.*[9] measured as-built shear strengths of 63 MPa on average, slightly above the average value of 46 MPa for 9 kW UAM as-built shear strengths measured. Studies by Obielodan *et al.*[10] using Cp Ti and Al 3003 exhibited as-built shear strengths of 34 MPa. Following a heat treatment of 480°C for 30 min, shear strengths of 73 MPa were measured while exhibiting diffusion of ~5 μm. This diffusion zone was said to provide solid solution strengthening at the interface, not present in the as-built samples. The study presented here proves that average shear strengths of 102 MPa are possible when using 9 kW UAM and a post-process heat treatment, which generates a similar 5 μm diffusion zone. However, in this case, the diffusion zone is believed to create a biaxial constraining action at the interface and associated strengthening as discussed by Truog.[6] The increased weld amplitude of 41.55 μm is expected to have increased the plastic deformation at the bond interfaces, thus increasing the driving force for recrystallisation at the interface and improving bonding as compared to the studies using 1 kW UAM. As-built samples in all three cases lack indications of diffusion, which, based on results of heat treated specimens, is necessary for maximising mechanical strength.

Electron backscatter diffraction of the as-built microstructure shows deformation in the aluminium layers, while the titanium appears unchanged. This is likely due to the deformation characteristics of each. The aluminium 1100 alloy is much weaker than the titanium layer, with ultimate tensile strengths of 90 and 343 MPa respectively.[11] Therefore, the much weaker aluminium layers are more likely to deform under load than the titanium layers. Upon heat treatment, the aluminium grains grow significantly, to the extent that each layer appears to contain only a few grains while the heat treatment does not appear to alter the grain structure of the titanium. The plastic deformation within the aluminium increases the driving force for recrystallisation to occur, and when heated to within 60°C of melting, recrystallisation and grain growth occur. Because there is little strain energy retained in the titanium from deformation and the heat treatment temperature is well below the melting temperature of titanium (1668°C), there is no driving force for recrystallisation to occur in the titanium layers. This preferential grain growth in the aluminium layers is consistent with previous research in Al 1100 alloys, where annealing treatments led to significant grain growth at temperatures approaching 600°C.[18]

Concluding remarks

Titanium–aluminium dissimilar material joints were achieved using 9 kW UAM. As-built and post-process heat treated samples were investigated for mechanical and microstructural properties. Heat treated samples show twofold increases in mechanical strength as compared to as-built samples for both push-pin and shear strength tests, achieving ultimate shear strengths over 100 MPa. Microstructural evaluations show no indications of voids or intermetallic formations in as-built samples and that the deformation and grain refinement is restricted to the aluminium layers. Diffusion of 5 μm and significant grain growth is seen in heat treated samples, and a small intermetallic layer is formed between the titanium and aluminium layers. This intermetallic layer is hypothesised as responsible for the increases in mechanical strength of the samples.

Acknowledgements

Funding for this work was provided by the Israeli Ministry of Defense. The authors would like to thank M. Norfolk of Fabrisonic LLC for providing technical support. Special thanks are given to D. Tung of the OSU Welding Engineering Program for his time and help in using the Gleeble 3800.

References

1. ASM International: 'Welding fundamentals and processes – ultrasonic additive manufacturing' **Vol. 6A**, 2011, Materials Park, OH, USA, ASM International.
2. R. Hahnlen and M. Dapino: 'NiTi–Al interface strength in ultrasonic additive manufacturing composites', *Composites B*, 2014, **59B**, 101–108.
3. C. Mou, P. Saffari, D. Li, K. Zhou, L. Zhang, R. Soar and I. Bennion: 'Smart structure sensors based on embedded fibre Bragg grating arrays in aluminium alloy matrix by ultrasonic consolidation', *Meas. Sci. Technol.*, 2009, **20**, 1–6.
4. M. Sriraman, M. Gonser, H. Fujii, S. Babu and M. Bloss: 'Thermal transients during processing of materials by very high power ultrasonic additive manufacturing', *J. Mater. Process. Technol.*, 2011, **211**, 1650–1657.
5. J. Obielodan, A. Ceylan, L. Murr and B. Stucker: 'Multi-material bonding in ultrasonic consolidation', *Rapid Prototyping J.*, 2010, **16**, (3), 180–188.
6. A. Truog: 'Bond Improvement of Al/Cu joints created by very high power ultrasonic additive manufacturing', Master's thesis, The Ohio State University, Columbus, OH, USA 2012.
7. P. Wolcott, A. Hehr and M. Dapino: 'Optimized welding parameters for Al 6061 ultrasonic additive manufactured structures', *J. Mater. Res.*, 2014, **29**, (27), 2055–2065.

8. C. Hopkins, P. Wolcott, M. Dapino, A. Truog, S. Babu and S. Fernandez: 'Optimizing ultrasonic additive manufactured Al 3003 properties with statistical modeling', *J. Eng. Mater. Technol.*, 2012, **134**, 011004-1–011004-10.
9. C. Hopkins, S. Fernandez and M. Dapino: 'Statistical characterization of ultrasonic additive manufacturing Ti/Al composites', *J. Eng. Mater. Technol.*, 2010, **132**, 041006-1–041006-9.
10. J. Obielodan, B. Stucker, E. Martinez, J. Martinez, D. Hernandez, D. Ramirez and L. Murr: 'Optimization of the shear strengths of ultrasonically consolidated Ti/Al 3003 dual-material structures', *J. Mater. Process. Technol.*, 2011, **211**, 988–995.
11. ASM International: 'Properties of wrought aluminum and aluminum alloys – properties and selection: nonferrous alloys and special-purpose materials' **Vol. 2**, 1992, Materials Park, OH, USA, ASM International.
12. A. Miriyev, A. Stern, E. Tuval, S. Kalabukhov, Z. Hooper and N. Frage: 'Titanium to steel joining by spark plasma sintering (SPS) technology', *J. Mater.Process. Technol.*, 2013, **213**, 161–166.
13. C. Zhang, A. Deceuster and L. Li: 'A method for bond strength evaluation for laminated structures with application to ultrasonic consolidation', *J. Mater. Eng. Perform.*, 2009, **18**, (8), 1124–1132.
14. Y. Kim and A. Fuji: 'Factors dominating joint characteristics in Ti–Al friction welds', *Sci.Technol.Weld.Join.*, 2002, **7**, (3), 149–154.
15. A. Fuji: 'Friction welding of Al–Mg–Si alloy to Ni–Cr–Mo low alloy steel', *Sci. Technol. Weld. Join.*, 2004, **9**, (1), 83–89.
16. M. Sloboda: 'Design and strength of brazed joints', 1961, London, Johnson Matthey Metals.
17. G. Heness, R. Wuhrer and W. Yeung: 'Interfacial strength development of roll-bonded aluminium/copper metal laminates', *Mater. Sci. Eng. A*, 2008, **A483–A484**, 740–742.
18. C. Kwan and Z. Wang: 'Microstructure evolution upon annealing of accumulative roll bonding (ARB) 1100 Al sheet materials: evolution of interface microstructures', *J. Mater. Sci.*, 2008, **43**, 5045–5051.